

Enhancement of Wear Resistance by β -Precipitates Formation on A7075/WC/ZrSiO₄ Surface Composites Fabricated Through FSP

Surendra Kumar Patel^{1*}, Avinash Ravi Raja¹, Sudesh Singh², Lei Shi¹

¹ MOE Key Lab for Liquid-Solid Structure Evolution and Materials Processing, Institute of Materials Joining, Shandong University, Jinan 250061, CHINA

² State Key Laboratory of Tribology in Advanced Equipment, Tsinghua University, Beijing, 100084, CHINA

*Corresponding Author: surendrakumarptl@gmail.com

DOI: <https://doi.org/10.30880/ijie.2024.16.02.002>

Article Info

Received: 19 September 2023

Accepted: 4 October 2023

Available online: 15 April 2024

Keywords

A7075 alloy, WC and ZrSiO₄ particles, wear, FSP, surface composite

Abstract

WC and ZrSiO₄ nanoparticle reinforced A7075 surface composites were fabricated using friction stir processing technique with 2, 4, and 6 passes. The microstructural analysis was performed by SEM, EDS, and XRD, which shows the better homogenous distribution of reinforcements into the A7075 surface matrix. The micro-hardness, tensile strength, and fatigue life were enhanced 60Hv, 167MPa, and 130000 cycles at 6 passes due to equally distributed formed β -precipitates over the surface. Similarly, the surface wear resistance also increases with increasing the processing passes. The improved processed surface properties were highly useful in the marine and aerospace industries.

1. Introduction

The reinforced microstructural, mechanical, and tribological properties of rich β -precipitates A7075 surface composite may be used in marine and aerospace industries [1]. However, the atomic compatibility of carbide and oxide reinforcements between the A7075 surface matrix enhanced the surface properties [2]. Additionally, the formation of intermetallic compounds (IMCs) into the A7075 alloy surface above the 400 °C by friction stir processing method plays an important role in improving the surface matrix properties [3, 4]. Hence, the IMCs at the surface matrix are presented in the form of β and α precipitates, which is responsible for increasing the surface wear resistance. [5]. So, the surface processing temperature and parameters must be the same for having good effects on β and α precipitates IMCs [6-7]. Whereas the surface durability of FSP composite thickness (1-6 mm) is reinforced with hexagonal particles which are used in aerospace and marine normally repaired [8].

Through the evolution of composite materials, the combination of properties and scopes has been, and is yet being, extended. In a broad aspect, a composite is regarded to be any material with a multi-phase that shows a significant combination of the characteristics of all component phases to offer enhanced aluminum surface properties [9]. This theory of combined action offers a superior mix of properties through the sensible blend of two or more predetermined materials. A composite is a multi-phase material that is made artificially. Besides, the components must be chemically different and isolated by a clear interface [10]. So, most alloys of metals and a lot of ceramics do not confine to this interpretation since these multiple phases are shaped as an outcome of the natural situation. Engineers and scientists have cunningly made compositions of various ceramics, and metals to fabricate a generation of the latest superior materials [11-15]. Most of them have been generated to enhance mechanical attributes such as toughness, stiffness, and strength at ambient and elevated temperatures. A great deal of them is constituted of simply two phases; one designated as matrix is ceaseless and envelops the other one

which is termed as the dispersed phase [16]. The characteristics of composites are a combination of the properties of constituent phases, their relative volume, and the dispersed phase geometry which includes shape, size, orientation, and distribution of the particles [17].

While a limited study on A7075/WC/ZrSiO₄ processed surface composite is available. Similarly, no studies carried out on β precipitates intermetallic compounds, which need to be studied for understanding the mechanism of A7075 and incorporated reinforcements into the surface. In the current research, the dual-reinforced defect-free A7075 surface composite was fabricated through the friction stir processing (FSP) method. Hence, the β precipitates intermetallic compounds such as ZrO₂, MgO₂, Al₂O₃, CuO₂, SiO₂, and WC, etc., enhanced the surface properties. Additionally, the improved surface properties of A7075 alloy are helpful for uses in the inner and outer aerospace surface as well as doors, ladder, and structural component in marine industries.

2. Experimental Details

The 7.5 wt.% WC and 7.5 wt.% ZrSiO₄ reinforcement were incorporated into A7075 surface composites using 2mm x 3mm grooves on 360mm x 60mm A7075 plate surface. The groove was made by a lathe machine and after filling the reinforcement into the groove, the groove was covered by a pin-less tungsten carbide tool through the FSW machine with a single pass. After that multi-pass surface composites were fabricated using pin tool (1200 rpm tool rotation and 60 mm/min tool traverse speed). The surface characterizations of the fabricated composite were analyzed by SEM, EDS, and XRD machines. Similarly, microhardness, tensile and fatigue test was performed on FH-10, MECH/UTE-40T as per ASTM D3479 standard test method. However, slurry abrasive and erosive wear test was performed on slurry abrasive tester-TR-44 and slurry erosive tester-TR-44. Furthermore, worn surface analysis was also done on slurry abrasive and erosive wear surfaces.

3. Results and Discussion

Figure 1(a-c) showed the SEM image of the A7075/WC/ZrSiO₄ friction-stirred composite at 2, 4 and 6 passes. A careful study shows that clusters of reinforced particles and generated kinds of β precipitates are distributed in the A7075 matrix as FSP pass increased. Figure 1(d-f) shows XRD patterns of ZrO₂, MgO₂, Al₂O₃, CuO₂, SiO₂, and WC intermetallic compound into A7075 friction-stirred surface composite at 2, 4 and 6 passes. All the diffraction peaks belong to the homogenous distribution over the surface in a single phase [18]. When grains re-refinement of the surface matrix occurs again and again, so β precipitates phase deboned with matrix and arises on the surface. Hence, at the 6th FSP passes the more homogenous β precipitates compound observed on the surface, which improved the surface wear resistance as revealed in Fig. 1(f). Similarly, Fig. 2 (a-c) shows EDS element mappings of Si, Zr, Mg, WC, Cr, Cu, Zn and Al signifying that all the elements are homogeneously dispersed in the A7075 surface composite.

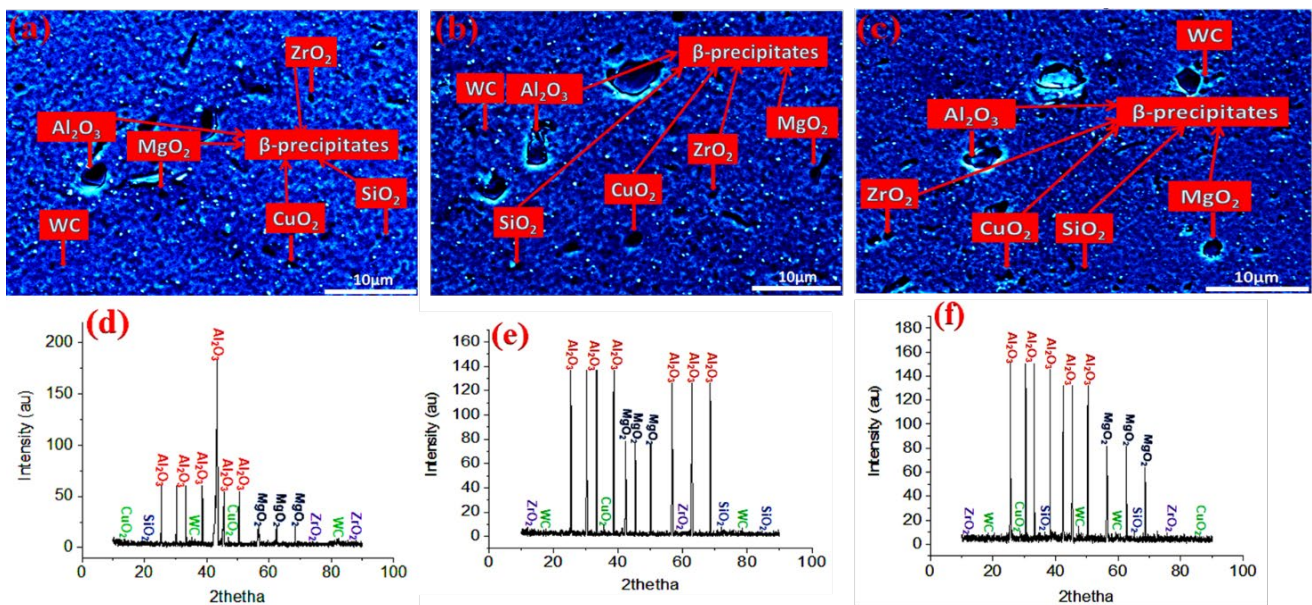
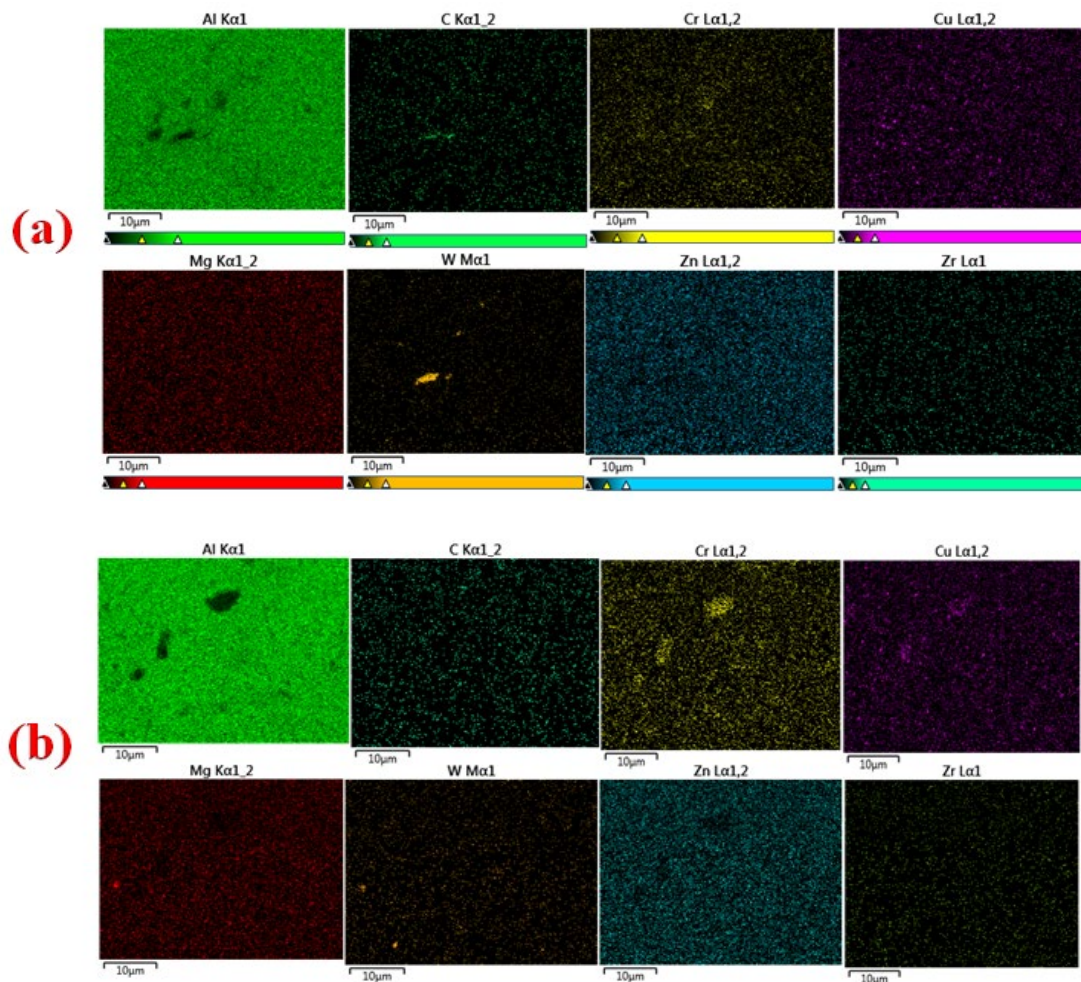


Fig. 1 SEM images (a) 2; (b) 4 and; (c) 6-pass; XRD patterns; (g) 2; (h) 4 and; (e) 6-pass of A7075/WC/ZrSiO₄ surface composite

Figure 3 (a-c) revealed, at 2, 4, and 6 FSP passes, the tensile strength of the FSP surface composite was improved to 400, 476, and 487 MPa, respectively. Improved surface properties like UTS, YS, elongation, and ductility were revealed by enriching interfacial bonding with reinforced $ZrSiO_4$ nanoparticles. The tensile property was improved with the presence of dendrites, which results in stress concentration points and strain for decreased tensile fracture nucleation or de-bonding [19]. Porosity was removed from the surface due to the dispersion of eutectic Si particles and the reformation of a continuous brittle Al_2O_3 network (fig. 3(a, b)) [20]. As depicted in fig 3(c), FSP caused the de-bonding of mutually coarse silicon interfaces and MgO_2 precipitates during compression, as well as the precipitation of intermetallic compounds made of ZrO_2 precipitates. the increased ductility improves the initial tensile deformation into the surface matrix.

The cyclic fatigue life of multi-FSP passes was tested at $25^\circ C$ temperature. Figures 4a (a1, a2), 4b (b1, b2), and 4c (c1, c2) show the fatigue life performance was improved by 52%, 67%, and 85% at 2, 4, and 6 FSP passes. Hence the increased fatigue life occurs due to precipitates hardening and slow crack growth on the surface (fig. 4c (c1, c2)). The stress fatigue life of the six FSP passes was much higher than the two and four passes. Additionally, 6 pass surfaces failed at 5kN load and 250000 cycle continuous stress amplitude. Dry conditions led to the lowest fatigue strength with increasing the processing passes deciphers into a higher cyclic loading procedure [21].



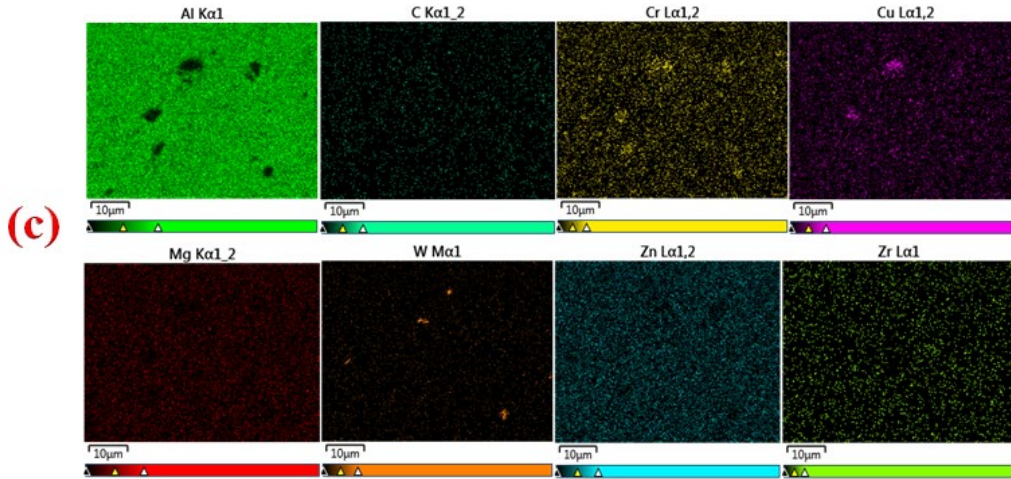
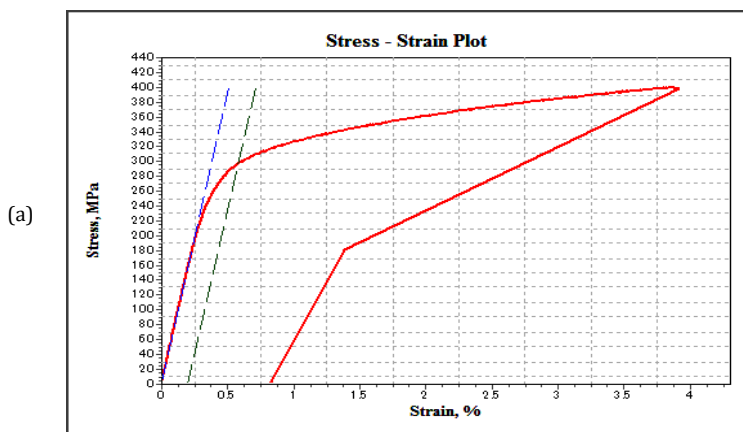


Fig. 2 EDS images (a) 2; (b) 4 and; (c) 6-pass of A7075/WC/ZrSiO4 surface composite

Fig. 5(b-d). The worn surfaces showed comparatively small grooves and slightly less plastically cut flank edges as increases FSP passes [22]. The craters were increased with increasing wheel hardness by 50 to 70 durometers on the worn-out surface due to the homogenous formation and distribution of intermetallic compounds in the A7075 matrix (fig. 5(b, c)). But at 6 FSP pass at 70 durometer slurry abrasive wear resistance was improved with β-precipitates intermetallic atomic matrix structure refinement and elimination of processing flaws including porosities 5(d).

The slurry erosive wear was conducted on time (3 hours), rotational speed (2000 rpm), and slurry (fine silica sand (20%), NaOH (4%)/HCL (1%), Tab water (75%)). The erosive wear occurs during sticking the slurry particles on the surface composite. The slurry erosive wear resistance was improved with increasing FSP passes as shown in Fig. 5(e). Because of the formation of metallic structures due to the increased temperature (250°C) of a slurry vessel as well as surface composite temperature [23]. As shown in Fig. 5(f-h), the worn morphology of slurry erosive wear was shown at 60% slurry concentration and 2000 rpm slurry rotation. The β-precipitates grains oppose the slurry sticking force in a slurry vessel, resulting in deep cuts and pitting being reduced on the composite surface [24]. The finer precipitates dispersed between the surfaces were opposed to mass loss during mechanical erosion wear (Fig. 5(g)). Furthermore, wear resistance increased due to formed atomic SiO₂, WC, and Al₂O₃ network layers to layers in interfusion formation into the worn surface (Fig. 5(h)).



Peak Stress	400.157 MPa
Peak Load	12.851 kN
0.2% Offset Yield Stress	297.565 MPa
Yield Strain	0.578 %
Yield Load	9.557 kN
Modulus	78.302 GPa
Elongation at Break (Using Strain)	0.834 %

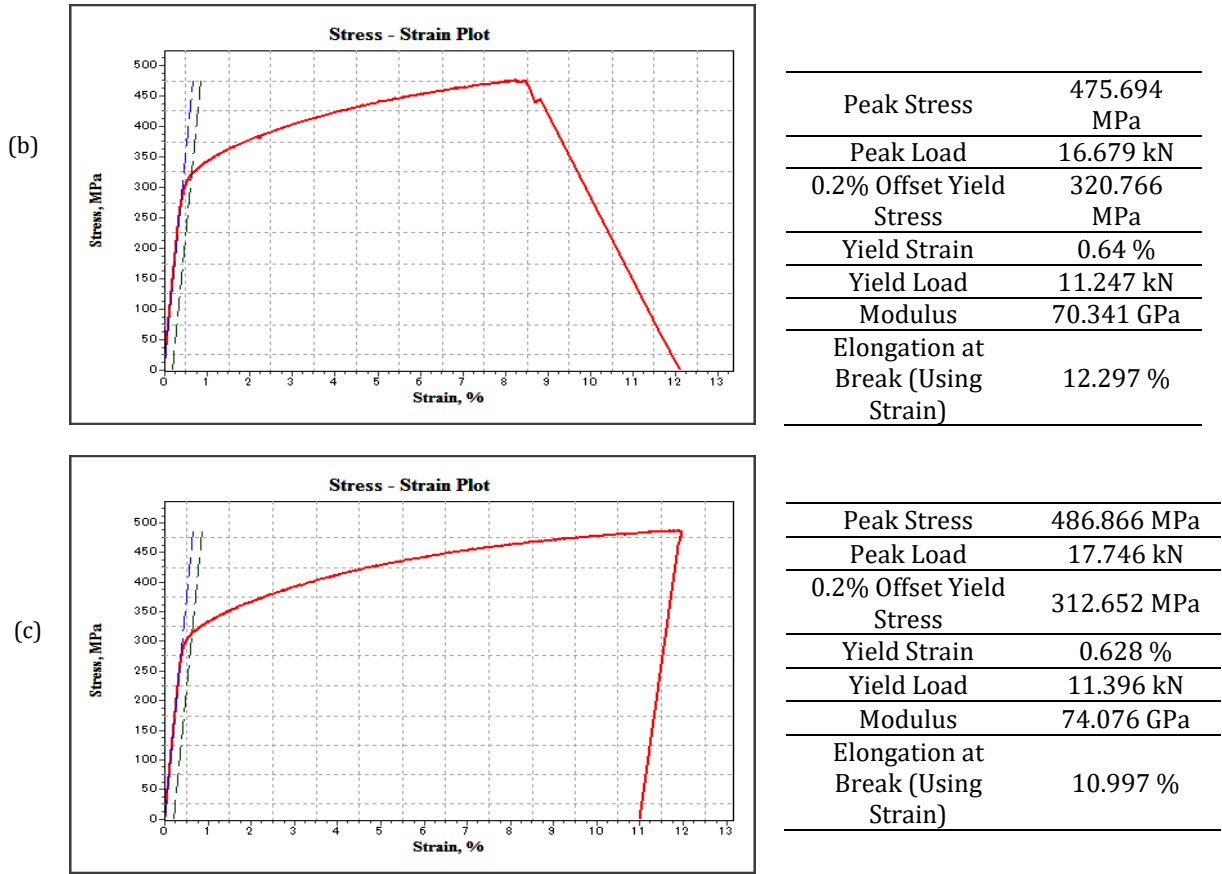
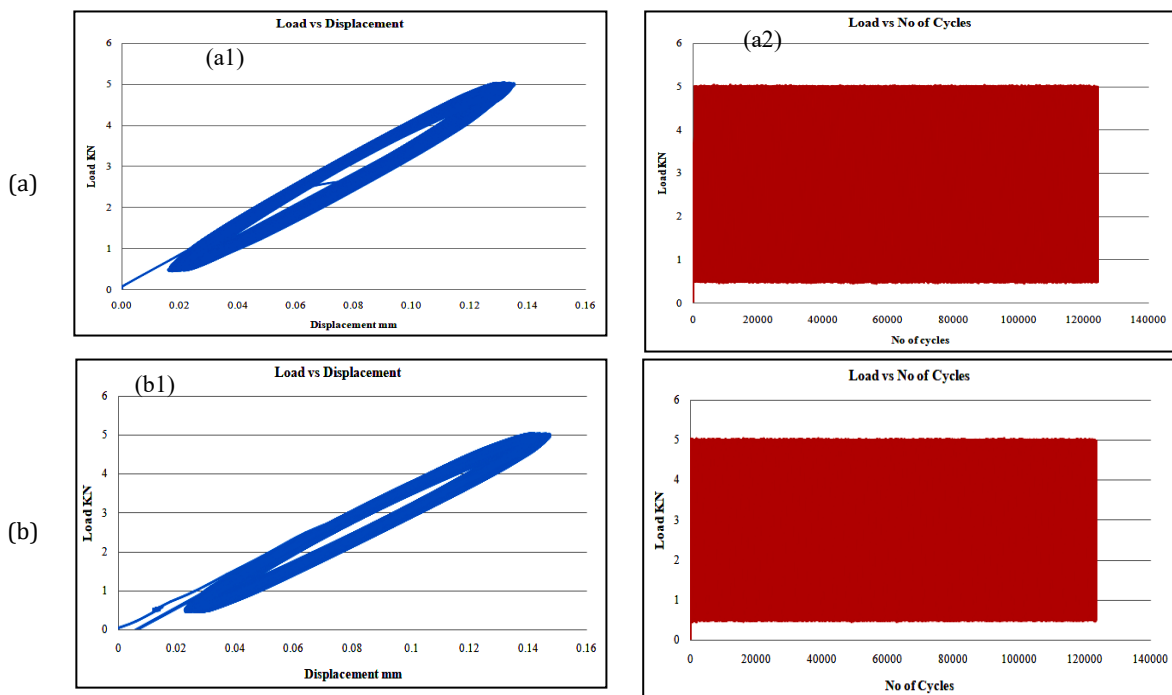


Fig. 3 Tensile properties of A7075/WC/ZrSiO₄ surface composite (a) 2; (b) 4, and; (c) 6-pass



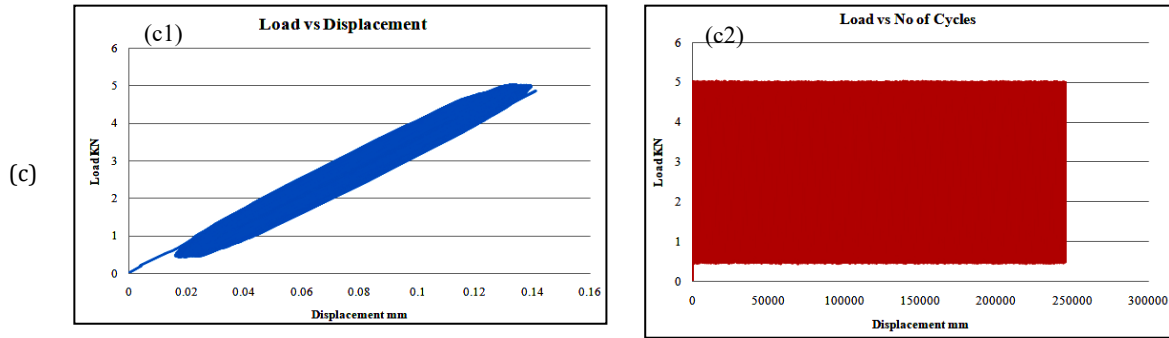
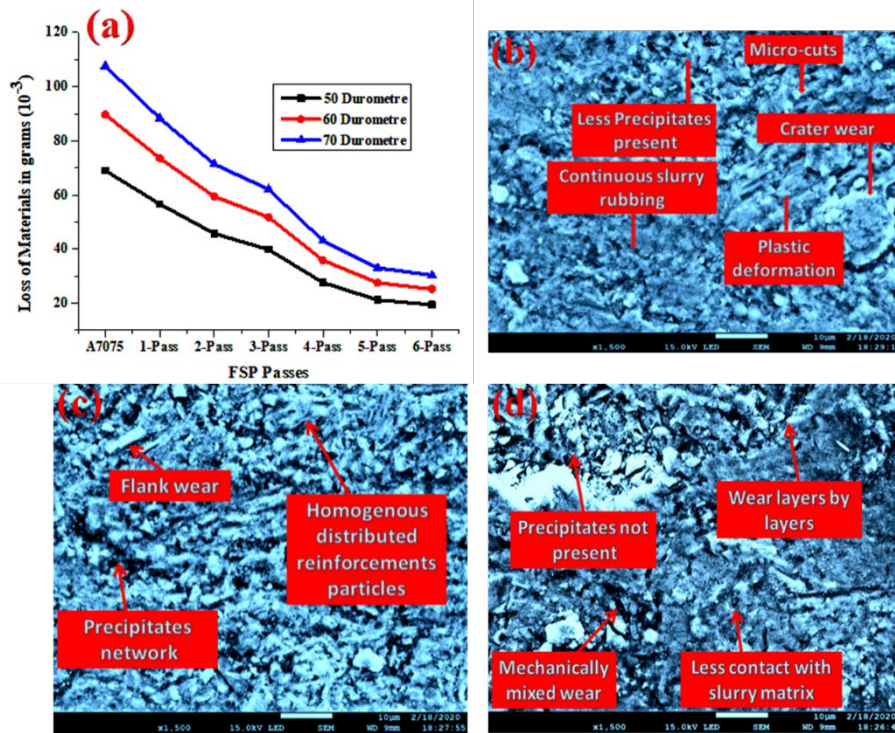


Fig. 4 Fatigue properties of A7075/WC/ZrSiO4 surface composite (a) 2-pass; (b) 4-pass; (c) 6-pass

4. Conclusions

The A7075 reinforced surfaces were fabricated smoothly by FSP technique. The microstructural results showed the homogeneous distribution of reinforcements and formed precipitates into surface matrix with increasing FSP passes. The grain size of the A7075-based surface composite with WC/ZrSiO4 reinforcement developed through FSP appeared to be more refined when compared to raw A7075 alloy. Results from SEM confirm the presence of WC/ZrSiO4 particles in the A7075 matrix in addition to improved bonding. The tensile strengths (UTS) were increased to 400, 476, 486 MPa and yield load was 9.5, 11.3 and 11.4 kN at 2, 4 and 6 passes. Which was resulted the precipitation hardening occurs at 4 and 6 FSP passes. The fatigue strength can affect by crystalline of precipitates into matrix. The precipitates doping significantly enhances the surface toughness which opposes the initial crack growth into surface matrix, so fatigue strength is enhanced with increasing processing passes. Furthermore, slurry abrasive and erosive wear resistance improved with increasing wheel hardness, slurry concentrations and FSP passes.



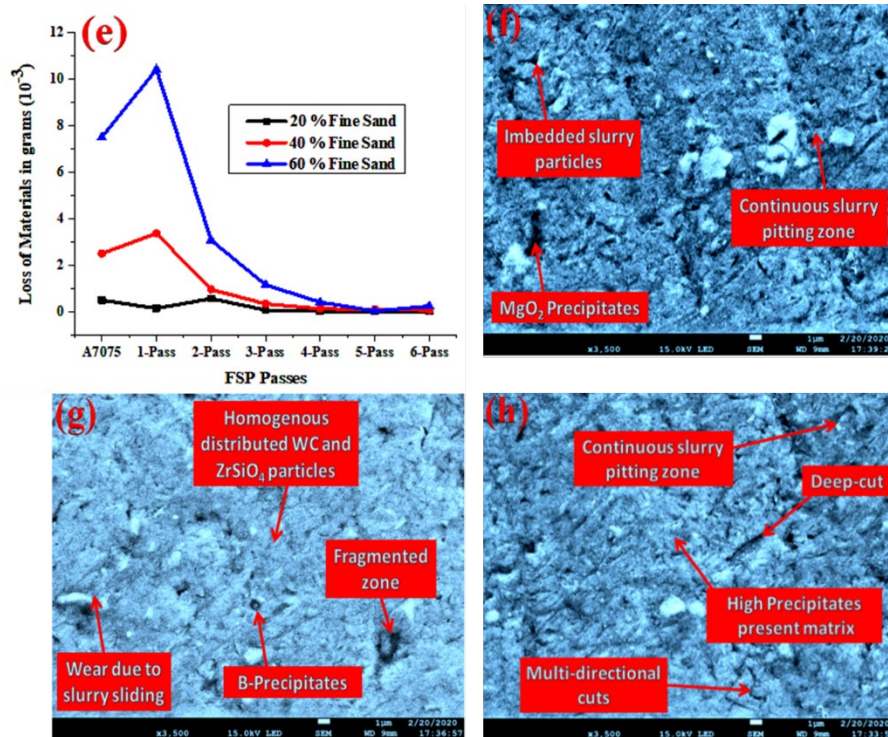


Fig. 5 (a) Slurry abrasive wear at 50, 60 and 70 durometers and worn SEM images at 6-pass; (b) 50; (c) 60; (d) 70 durometer; (e) slurry erosive wear at 2000 rpm at 60% slurry concentration and worn images; (f) 2-pass; (g) 4-pass; (h) 6-pass of A7075/WC/ZrSiO₄ surface composite

Acknowledgement

The authors fully acknowledged Shandong University and Tsinghua University for supporting this work.

Conflict of Interest

Authors declare that there is no conflict of interests regarding the publication of the paper.

References

- [1] Mishra, R. S., Mahoney, M. W., McFadden, S. X., Mara, N. A., & Mukherjee, A. K. (1999). High strain rate superplasticity in a friction stir processed 7075 Al alloy. *Scripta materialia*, 42(2), 163-168.
- [2] Moustafa, E. B., Melaibari, A., & Basha, M. (2020). Wear and microhardness behaviors of AA7075/SiC-BN hybrid nanocomposite surfaces fabricated by friction stir processing. *Ceramics International*, 46(10), 16938-16943.
- [3] Mishra, R. S., Ma, Z. M. (2005). Friction stir welding and processing, *Mater. Sci. Eng. R. Reports*.50 (1-2), 1-78.
- [4] Tang, J., Shen, Y., & Li, J. (2019). Influences of friction stir processing parameters on microstructure and mechanical properties of SiC/Al composites fabricated by multi-pin tool. *Journal of Manufacturing Processes*, 38, 279-289.
- [5] Sabbaghian, M., Shamanian, M., Akramifard, H. R., & Esmailzadeh, M. (2014). Effect of friction stir processing on the microstructure and mechanical properties of Cu-TiC composite. *Ceramics International*, 40(8), 12969-12976.
- [6] Mirjavadi, S. S., Alipour, M., Hamouda, A. M. S., Matin, A., Kord, S., Afshari, B. M., & Koppad, P. G. (2017). Effect of multi-pass friction stir processing on the microstructure, mechanical and wear properties of AA5083/ZrO₂ nanocomposites. *Journal of Alloys and Compounds*, 726, 1262-1273.
- [7] Mishra, R. S., Ma, Z. Y., & Charit, I. (2003). Friction stir processing: a novel technique for fabrication of surface composite. *Materials Science and Engineering: A*, 341(1-2), 307-310.
- [8] Ni, D. R., Wang, J. J., Zhou, Z. N., & Ma, Z. Y. (2014). Fabrication and mechanical properties of bulk NiTip/Al composites prepared by friction stir processing. *Journal of Alloys and Compounds*, 586, 368-374.
- [9] Jalilvand, M. M., & Mazaheri, Y. (2020). Effect of mono and hybrid ceramic reinforcement particles on the tribological behavior of the AZ31 matrix surface composites developed by friction stir processing. *Ceramics International*, 46(12), 20345-20356.

- [10] Singh, V. P., Patel, S. K., Ranjan, A., & Kuriachen, B. (2020). Recent research progress in solid state friction-stir welding of aluminium–magnesium alloys: a critical review. *Journal of Materials Research and Technology*, 9(3), 6217-6256.
- [11] Wu, N., Xue, F., He, J., Wang, C., Lu, J., Zhou, H., ... & Luo, F. (2022). Effect of tungsten carbide content on the tribological behavior of TiB₂–TiC-based cermets. *Wear*, 498, 204333.
- [12] Huang, G., & Shen, Y. (2017). The effects of processing environments on the microstructure and mechanical properties of the Ti/5083Al composites produced by friction stir processing. *Journal of Manufacturing Processes*, 30, 361-373.
- [13] Zhou, D., Qiu, F., & Jiang, Q. (2015). The nano-sized TiC particle reinforced Al–Cu matrix composite with superior tensile ductility. *Materials Science and Engineering: A*, 622, 189-193.
- [14] Saenz-Betancourt, C. C., Rodríguez, S. A., & Coronado, J. J. (2022). Effect of boronising on the cavitation erosion resistance of stainless steel used for hydromachinery applications. *Wear*, 498, 204330.
- [15] Zuo, L., Shao, W., Zhang, X., & Zuo, D. (2022). Investigation on tool wear in friction stir welding of SiCp/Al composites. *Wear*, 498, 204331.
- [16] Zum Gahr, K. H. (1998). Wear by hard particles. *Tribology International*, 31(10), 587-596.
- [17] Jiang, H., Winder, D., McClintock, D., Bruce, D., Schwartz, R., Kyte, M., & Carroll, T. (2022). Quantifying the reduction in cavitation-induced erosion damage in the Spallation Neutron Source mercury target by means of small-bubble gas injection. *Wear*, 496, 204289.
- [18] Javaheri, V., Sadeghpour, S., Karjalainen, P., Lindroos, M., Haiko, O., Sarmadi, N., ... & Kömi, J. (2022). Formation of nanostructured surface layer, the white layer, through solid particles impingement during slurry erosion in a martensitic medium-carbon steel. *Wear*, 496, 204301.
- [19] Qian, J., Li, J., Xiong, J., Zhang, F., & Lin, X. (2012). In situ synthesizing Al₃Ni for fabrication of intermetallic-reinforced aluminum alloy composites by friction stir processing. *Materials Science and Engineering: A*, 550, 279-285.
- [20] Selvakumar, S., Dinaharan, I., Palanivel, R., & Babu, B. G. (2017). Characterization of molybdenum particles reinforced Al6082 aluminum matrix composites with improved ductility produced using friction stir processing. *Materials Characterization*, 125, 13-22.
- [21] Li, J., Qiu, H., Zhang, X. F., Yu, H. L., Yang, J. J., Tu, X. H., & Li, W. (2022). Effects of (Ti, Mo) C particles on the abrasive wear-corrosion of low alloy martensitic steel. *Wear*, 496, 204288.
- [22] Hu, Y., Pan, J., Dai, Q., Huang, W., & Wang, X. (2022). Solid particle erosion-wear behaviour of SiC particle-reinforced Si matrix composite and neat Si—A comparison. *Wear*, 496, 204286.
- [23] Kumar, A., Pal, K., & Mula, S. (2017). Simultaneous improvement of mechanical strength, ductility and corrosion resistance of stir cast Al7075-2% SiC micro-and nanocomposites by friction stir processing. *Journal of Manufacturing Processes*, 30, 1-13.
- [24] Li, Z. Y., Cai, Z. B., Zhang, W., Liu, R. R., Yang, Z. B., & Jiao, Y. J. (2022). Effect of coolant pH on the fretting corrosion behavior of zirconium alloy. *Wear*, 496, 204269.